

Influence of the elastic mismatch on the Hertzian cone crack path in ceramic bilayers

L. Ceseracciu^a, M. Anglada^b, E. Jiménez-Piqué^{b,c,*}

^a *Istituto Italiano di Tecnologia, Nanophysics, via Morego 30, 16163 Genova, Italy*

^b *Universitat Politècnica de Catalunya, Department of Materials Science and Metallurgical Engineering, Av. Diagonal, 647, 08028 Barcelona, Spain*

^c *Center for Research in Nano-engineering, CRNE, C/ Pascual i Vila, 15, 08028 Barcelona, Spain*

Received 1 February 2011; received in revised form 6 April 2011; accepted 25 April 2011

Available online 20 May 2011

Abstract

Contact damage is a key aspect in the structural integrity of ceramics, particularly ceramic coatings and multilayers that may have an elastic mismatch. An understanding of the critical load and trajectories of the crack produced by contact loads in such materials is valuable to characterize the damage tolerance and improve their reliability. In this work, the Hertzian cone crack initiation and propagation in brittle bilayers has been studied by FEM and verified by experimental observations. It was concluded that the elastic mismatch affects the crack initiation position and critical load for cone cracking. Critical loads are lower in bilayers than in monolithic materials. Cone crack trajectory and the corresponding fracture energy release rate are also affected by the elastic mismatch, which thus influences the damage tolerance of the system.

© 2011 Elsevier Ltd. All rights reserved.

Keywords: Indentation; Fracture; Hardness; Mechanical properties; Surfaces

1. Introduction

Ceramic materials present interesting mechanical properties for surface loading applications such as high hardness, wear resistance, chemical inertness and high stiffness. However their intrinsic brittleness makes them sensitive to small flaws. Since fracture is controlled by the size of natural crack-like defects, this translates into a large scatter in the strength and low reliability in service. In order to overcome such a weakness, one strategy is to use ceramics as surface layers, either on a tougher substrate or in multilayer architectures. Multilayered ceramics improve the damage tolerance, for example, by crack deflection,^{1,2} residual stresses,^{3–6} phase transformation⁷ or porosity.⁸ Thanks to their enhanced mechanical properties, ceramic multilayers can be employed in structural applications, even where severe loadings can be expected. Among these, the most common ones exploit the other good properties of

ceramics, such as wear resistance, and therefore involve contact loading.

Contact loading in brittle materials, while not being the usual final cause of failure in components, produce damage and cracks in the material which act as initial flaws for subsequent crack propagation and ultimate fracture.^{9,10} Very often, contact loading takes place by a blunt contact, and the usual framework to study such type of damage is by Hertzian indentation,¹¹ either with a sphere or a flat punch.¹² The inhomogeneous, high-graded stress field generated in Hertzian indentation represents satisfactorily the contact loading in service. It is worth mentioning that indentation techniques can also be used for extracting local properties of materials since they probe small volumes of materials.

Damage produced by such type of loading on monolithic materials can be classified as brittle or quasi-plastic, the former being characterized by ring-cone cracking starting from the contact zone,^{11,13} the latter by inelastic deformation by shear-driven microcracking beneath the indenter.¹⁴

In layered materials, the monolithic contact stress field is modified by the presence of the residual stress field and by the presence of interfaces which give rise to a number of modes of damage, which can start at different locations: (a) from the surface as a ring crack,¹⁵ as in the monolithic case, or as a remote

* Corresponding author at: Universitat Politècnica de Catalunya, Department of Materials Science and Metallurgical Engineering, Av. Diagonal, 647, 08028 Barcelona, Spain. Tel.: +34 934011089.

E-mail address: emilio.jimenez@upc.edu (E. Jiménez-Piqué).

ring, due to the stress field modification; (b) at the interface as radial cracks; (c) within either the substrate or the coating as plastic or quasi-plastic yield.¹⁶ An excellent analysis of the radial and remote-cone cracks initiation was presented by Chai.¹⁷

Recent studies have proved that laminated materials present an enhanced resistance to contact loading, both under static and cyclic loadings.^{13,18} In terms of fracture mechanics, it has also been shown that the cone crack angle and length may be severely modified in these materials compared to monolithic ceramics, both by the *R*-curve behaviour and the residual stresses.¹⁹ It is thought that even in absence of such phenomena, the mere elastic mismatch between the first and second layer may have a remarkable influence on the crack formation.

In this work, we have studied the effect of the elastic mismatch between an upper brittle layer (labelled as coating) of a thickness in the order of magnitude of the contact diameter and a second layer (labelled as substrate) on the critical load for ring-cone crack formation and on the crack path.

This was carried out by means of an automated Finite Element model of crack propagation, described in detail elsewhere.¹⁹ A flat-punch indentation was applied to coatings of thickness approximately half the indenter radius, and with an either stiffer or more compliant substrate. The critical load for ring crack formation, its initial radius and growth stability, and the cone crack propagation inside the coating are affected by the stress modification. The values and considerations inferred by simulations were verified by experimental observations on a model material of glass stacked on either alumina or PMMA. The objective of the study was to analyse the influence induced by such cracks on the damage tolerance of the component.

2. Experimental procedure

Flat punch indentation was performed on a universal testing machine, with a WC-Co 2.5 mm-radius indenter on two bilayer composites, consisting of a 1 mm thick glass layer, referred to as “coating layer” (Young’s modulus $E_c = 72$ GPa, Poisson’s ratio $\nu_c = 0.18$), and either a stiff substrate of alumina ($E_s = 380$ GPa, $\nu_s = 0.25$) or a compliant substrate of PMMA ($E_s = 3$ GPa and $\nu_s = 0.3$), for E_c/E_s ratios of 0.19 and 24, respectively. The output of the test was the critical indentation load for the appearance of the first crack, determined through an iterative procedure; the crack radius was measured after the test with an optical microscope.

Finite Element simulation was carried out by means of an automatic model of crack propagation, whose details are reported elsewhere,¹⁹ created on the commercial software ABAQUS, version 6.7, powered by the use of the built-in programming code Python. A model of the studied systems was created automatically based on the input geometry, the appropriate boundary conditions were applied, and the mesh was generated automatically. The mesh was highly inhomogeneous, finer in the zones of higher stress gradient, at the contact zone and at the crack tip. Such local refinement was obtained through a 3-to-1 elements transition. A short crack (typically 7 μm long) was placed close to the contact area, and flat punch indentation was simulated by vertical displacement of the nodes corresponding

to the contact zone. The corresponding indentation load was calculated from the reaction force at the same nodes. The fracture energy release rate G and the stress intensity factors K_I , K_{II} were calculated at the crack tip from a contour integration, as a direct output of the software. For a general approach, the substrate Young’s modulus was considered a parameter, ranging from 9 to 1728 GPa, so that the E_c/E_s ratio varied between 0.125 and 24.

The analysis followed two steps: the initial radius and critical load for each value of E_c/E_s were determined by varying the former and finding the location of highest fracture energy release. Since the model assumes purely elastic materials, it was possible to calculate the corresponding indentation load indirectly after one simulation, following the approximate relation

$$\frac{P_c}{P} \propto \sqrt{\frac{G_c}{G}} \quad (1)$$

The critical fracture energy was taken as $G_c = 9.5 \text{ Jm}^{-2}$, as calculated from the known fracture toughness by means of the known relation:

$$G_c = \frac{K_{Ic}^2}{E} (1 - \nu^2) \quad (2)$$

The initial radius and load thus calculated were used for simulation of crack propagation. The model described above was updated iteratively with small increments of the crack length along the kinking direction, defined²⁰ as

$$\beta = -2 \frac{K_{II}}{K_I} \quad (3)$$

Crack propagation was carried on until the crack tip was at a short distance from the interface, where the contour integration would have been ill defined.

The accuracy of the comparison with experiments was hindered by the simplification of assuming only brittle cracking in the simulations, but this on one hand is not unreasonable, because all the materials chosen present prevalently brittle fracture, and on the other hand was necessary for the sake of simplicity.

3. Results and discussion

Crack formation and growth under blunt contact is caused by tensile stress near the indentation area. The presence of a substrate with a different Young’s modulus from the coating modifies the peak values of such tensile stress and its location, because a redistribution of the stress field takes place towards the stiffer layer. The consequence is that, both the critical load necessary for the surface ring crack formation and the corresponding initial crack radius are modified. This is confirmed by the simulations of crack initiation, shown in Fig. 1, where the critical load necessary for cone crack propagation (i.e. to fulfil the relation $G > G_c$) is shown as a function of the starting radius for several E_c/E_s ratios. A summary of the results is presented in Fig. 2 in terms of this latter parameter. It can be seen that the lowest loads correspond to the highest E_c/E_s ratios,

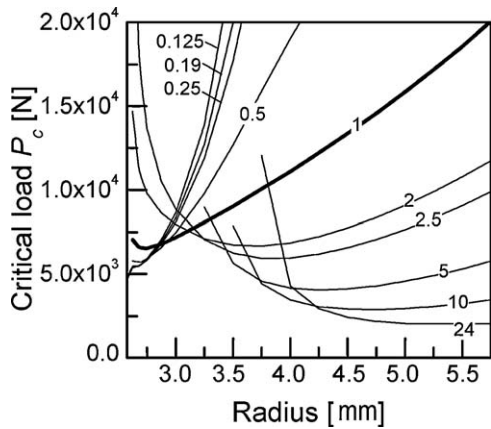


Fig. 1. Critical load necessary for crack propagation as a function of the starting position, assuming a $7 \mu\text{m}$ long initial defect, for values of E_c/E_s ranging from 0.125 to 24. The bold curve indicates the case of homogeneous material.

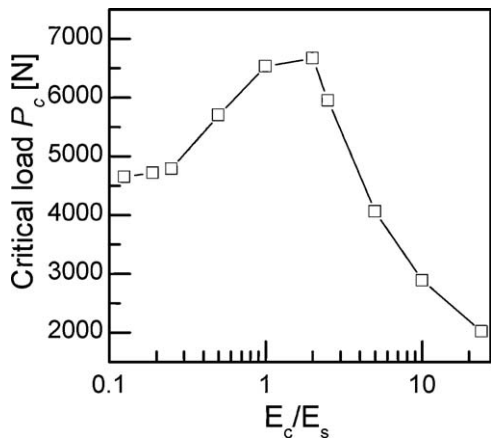


Fig. 2. Critical load for cone crack formation as a function of the E_c/E_s ratio.

as could be expected from the larger compliance of the substrate, which causes a bending-like deformation of the indented layer¹⁶; however, as E_c/E_s becomes smaller than one, the critical load becomes lower again. This is attributed to the constraint induced by the stiff substrate, which concentrates the stress near the contact zone.

Experimental measurements of the critical load were in agreement with the predicted values, as shown in Table 1. The trend of crack starting position variation was also confirmed, although with some difference in the absolute values. Typical cracks from both systems are shown in Fig. 3, where the presence of other crack systems can be seen, especially in the glass/ Al_2O_3 bilayer, which are thought to be the reason for the mentioned discrepancy.

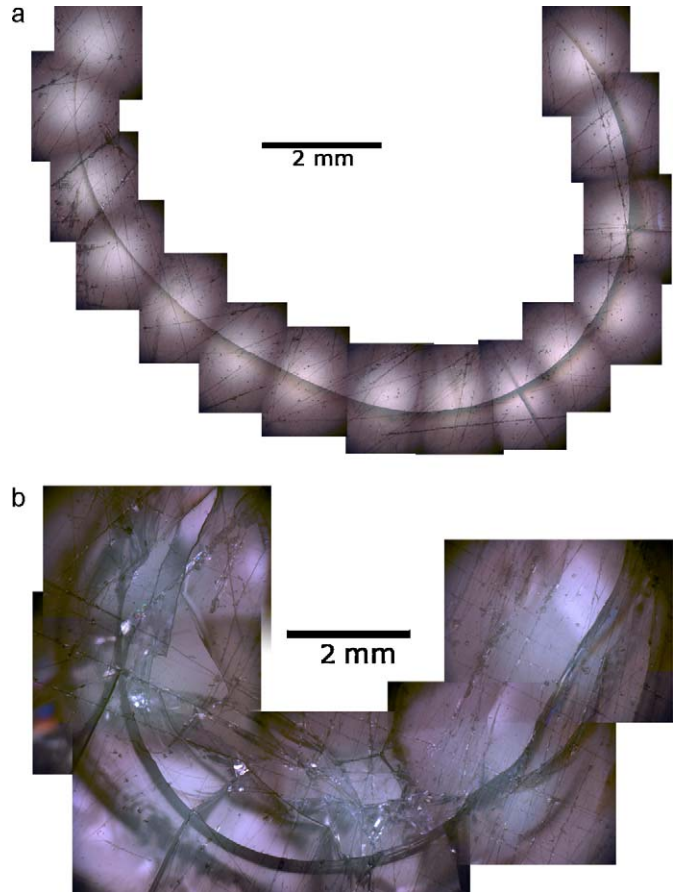


Fig. 3. Typical ring cracks (a) in the glass/PMMA bilayer and (b) in the glass/ Al_2O_3 bilayer.

The crack geometry is affected by the elastic mismatch, as it can be seen in Fig. 4, where the crack trajectories are presented for the studied range of the elastic mismatch. Although the results are slightly dependant on the initial crack size assumed, there is a transition from the classical cone crack on monolithic materials, with initial radius close to the contact area, to a “remote cone crack” as the substrate elastic modulus decreases, which has been already reported before.¹⁷ The different geometry is attributed to the stress field: the first principal stress trajectories are almost parallel to the surface far from the indented zone, so that the first propagation is almost straight, and the outward curvature begins when the crack approaches the layers interface, due in this case to the elastic mismatch. Elastic mismatch is also responsible of the geometry variation for low values of E_c/E_s : although the crack starting radius is almost the same for values from 0.125 to 0.5, a strong deviation from the classical constant-angle geometry can be observed for

Table 1

Experimental and numerical critical load for the appearance of ring crack and corresponding initial crack radius, for the studied systems.

	E_c/E_s	P_c [N]		r [μm]	
		Exp	FE	Exp	FE
Glass/PMMA	0.19	1450	2017	3040 ± 56	2625
Glass/ Al_2O_3	24	5650	5417	4370 ± 602	5250

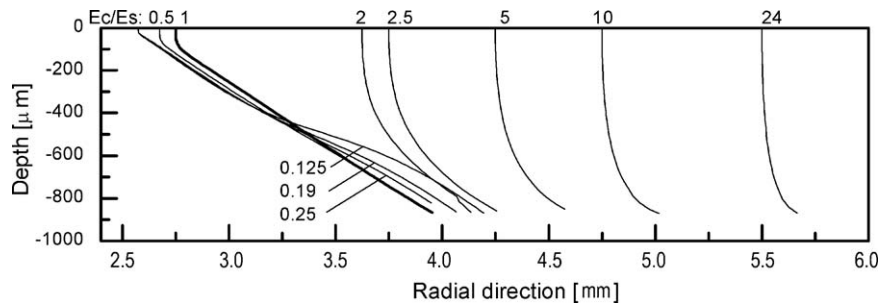


Fig. 4. Cone crack trajectories corresponding to values of the ratio E_c/E_s ranging from 0.125 to 24. The bold curve indicates the case of homogeneous material.

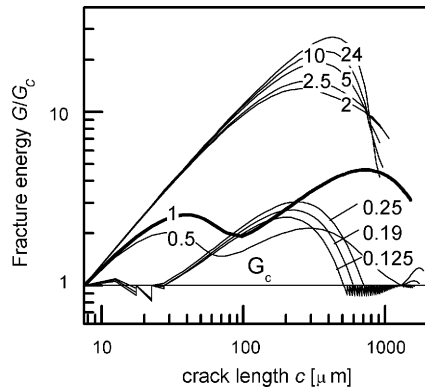


Fig. 5. Fracture energy released throughout the crack propagation for several values of the E_c/E_s ratio, as reported in the figure. The bold curve indicates the case of homogeneous material.

long-enough cracks, with a kink at approximately half the coating thickness, kink that is more pronounced as the mismatch is larger.

The fracture energy release rate, normalized against the critical value G_c necessary for crack propagation, is shown in Fig. 5 as a function of the crack length. Whenever the energy released was lower than the critical value, a small load increment was applied to produce stable growth, which results in saw-shaped regions.

For $E_c/E_s > 1$ (stiffer coating), the behaviour is different with respect to the classical cone crack, since the classical 4-branched shape²¹ is absent. Instead, there is only one maximum, so that propagation is unstable throughout the straight portion, while the successive energy drop is associated with the change in the path angle shown in Fig. 4.

A different behaviour can be seen for the lower values of E_c/E_s . Because of the reduced starting radius, the ring-shaped portion of the crack is shallower, and G_c is lower, falling soon below the critical value, so that the crack propagation becomes stable. An unstable branch follows, until, similarly to the $E_c/E_s > 1$ case, grows smaller and falls again below G_c when the crack approaches the substrate.

4. Conclusions

A Finite Element study was conducted to study the influence of the elastic mismatch on the response to Hertzian indentation of brittle bilayers. The cone crack generated by flat punch

indentation was simulated by means of an automated model of crack propagation, and the following considerations on the influence on damage tolerance were drawn:

1. Both a compliant and a stiff substrate reduce the critical load for ring cracking of a brittle coating, compared to the same material taken as a monolith, or to a coating much thicker than the indenter diameter.
2. As E_c/E_s increases, the cone crack geometry changes towards a remote cone configuration which, because of its unstable propagation, can be immediately detrimental for the structural integrity of the component. In addition, the crack angle is much higher (i.e. the crack is perpendicular to the surface), which may result in a more harmful initial flaw, for a given crack length.
3. Low values of E_c/E_s , despite favouring fracture initiation, improve the resistance to cone crack propagation, because of two stable branches at both short and long crack length. Therefore, although less resistant to initial growth of a flaw produced by contact loading, low values of E_c/E_s will produce short, detectable cone cracks with a lower angle which will be less harmful to the structural integrity of the component.

Acknowledgements

Work supported in part by Ministerio de Ciencia e Innovación of Spain through Projects MAT2008-03398/MAT and MAT 2006-13480/MAT and by the Generalitat de Catalunya (2009SGR01285).

References

1. Sanchez-Herencia AJ, Pascual C, He J, Lange FF. ZrO₂/ZrO₂ layered composites for crack bifurcation. *J Am Ceram Soc* 1999;**82**: 1512–8.
2. Clegg W, Kendall K, Alford N, Button TW, Birchall JD. A simple way to make tough ceramics. *Nature* 1990;**347**:455–7.
3. Chan HM. Layered ceramics: processing and mechanical behavior. *Annu Rev Mater Sci* 1997;**27**:249–82.
4. Bermejo R, Torres Y, Sanchez-Herencia AJ, Baudín C, Anglada M, Llanes L. *Acta Mater* 2006;**54**:4745–57.
5. Virkar AV, Jue JF, Hansen JJ, Cutler RA. Measurement of residual-stresses in oxide-ZrO₂ 3-layer composites. *J Am Ceram Soc* 1998;**71**:C148–51.
6. Bermejo R, Ceseracciu L, Llanes L, Anglada M. *Key Eng Mater* 2009;**409**:94–106.

7. Sanchez-Herencia AJ, James L, Lange FF. Bifurcation in alumina plates produced by a phase transformation in central alumina/zirconia thin layers. *J Eur Ceram Soc* 2000;**20**(9):1297–300.
8. Sorensen BF, Horsewell A. Crack growth along interfaces in porous ceramic layers. *J Am Ceram Soc* 2001;**84**:2051–9.
9. Ceseracciu L, Jimenez-Pique E, Fett T, Anglada M. Contact strength of ceramic laminates. *Compos Sci Technol* 2008;**68**:209–14.
10. Kim D, Jung Y, Peterson I, Lawn B. Cyclic fatigue of intrinsically brittle ceramics in contact with spheres. *Acta Mater* 1999;**47**:4711–25.
11. Lawn BR. Indentation of ceramics with spheres: a century after Hertz. *J Am Ceram Soc* 1998;**81**:1977–94.
12. Mougnot R, Maugis D. Fracture indentation beneath flat and spherical punches. *J Mater Sci* 1985;**20**:4354–76.
13. Jiménez-Piqué E, Ceseracciu L, Chalvet F, Anglada M., de Portu G. Hertzian contact fatigue on alumina/alumina–zirconia laminated composites. *J Eur Ceram Soc* 2005;**25**:3393–401.
14. Lawn BR, Padture MP, Cai H, Guiberteau F. Making ceramics ductile. *Science* 1994;**263**:1114–6.
15. Pavón J, Jiménez-Piqué E, Anglada M, Saiz E, Tomsia AP. Monotonic and cyclic Hertzian fracture of a glass coating on titanium-based implants. *Acta Mater* 2006;**54**:3593–603.
16. Miranda P, Pajares A, Guiberteau F, Deng Y, Lawn BR. Designing damage-resistant brittle-coating structures: I. Bilayers. *Acta Mater* 2003;**51**:4347–56.
17. Chai H. Crack propagation in glass coatings under expanding spherical contact. *J Mech Phys Solids* 2006;**54**:447–66.
18. Ceseracciu L, Chalvet F, de Portu G, Anglada M, Jimenez-Pique E. Surface contact degradation of multilayer ceramics under cyclic subcritical loads and high number of cycles. *Int J Refract Met Hard Mater* 2005;**23**:375–81.
19. Ceseracciu L, Anglada M, Jimenez-Pique E. Hertzian cone crack propagation on polycrystalline materials: role of R-curve and residual stresses. *Acta Mater* 2008;**56**:265–73.
20. Cotterell B, Rice JR. Slightly curved or kinked cracks. *Int J Fract* 1980;**16**:155–69.
21. Lawn BR. *Fracture of brittle solids*. Cambridge, UK: Cambridge University Press; 1993.